

SOME RESULTS OF ANALYSIS OF OSCILLOGRAMS OF THE  
INSTANTANEOUS THICKNESS OF A LIQUID FILM IN A  
DISPERSED-ANGULAR FLOW

N. D. Agafonova and M. A. Gotovskii

UDC 532.551.011.18:621.18

Data was obtained on the distribution of the thickness of a film and the amplitude of waves on its surface.

Information can be obtained on wave formation on the surface of a liquid film in a dispersed-annular flow by analyzing oscillograms of the instantaneous thickness of the film. One of the analytical methods currently being used is calculation of the autocovariation function and power spectrum of the wave process, with determination of the frequencies of harmonic oscillation. Another method consists of constructing the film-thickness distribution function, which makes it possible to determine the amplitude characteristics of the surface of the liquid.

The study [1] presented a description of a unit and method of measurement and examined results of the use of spectral analysis to interpret experimental data on the thickness of a liquid film in a dispersed-annular flow. Oscillograms of instantaneous film thickness were obtained for an air-water flow ascending in a vertical pipe 16 mm in diameter. The investigators used electrical conductivity sensors to obtain their data. The regime parameters were varied within the range: water flow rate  $G_q = (4-35) \cdot 10^{-3}$  kg/sec, air flow rate  $W_g = 15-43$  m/sec. The pressure in the loop was close to atmospheric.

Here we report results of analysis of oscillograms of film thickness performed with histograms. The initial material was a sample of 1000 values of the instantaneous thickness of the film  $h$  determined at time intervals of 0.5 msec. Here, the number of intervals for one grouping  $k$  was chosen so that the incidence of the data in each interval would be at least two (except for the extreme intervals) [2]. It is evident that the value of  $k$  depends on the range and the error of the characteristic being determined (film thickness in the present case). The mean thickness of the film changed in the tests from 0.055 to 0.3 mm, depending on the regime parameters. The error of the determination of instantaneous film thickness with electrical conductivity sensors depends on the parameters of the sensor, the amplification scheme, and the choice of rate when recording the signal from the sensor on the photographic paper of the oscillograph. Also playing an important role is the calibration curve, which determines the relationship between the electrical signal of the sensor and the film thickness. The error of the film-thickness determination did not exceed 15% for instantaneous film-thickness values  $h \geq 0.8$  mm, while it ranged from 6 to 9% at  $h < 0.8$  and was the criterion for the selection of the grouping interval (this interval should not be less than the error of  $h$ ). In the analysis of the tests,  $k$  took values of 8-15.

The distribution functions of film thickness constructed from histograms generally turned out to be nonsymmetrical relative to the abscissa of the maximum, as is apparent from Fig. 1. The functions also travelled a smoother path in the region of large thicknesses. As is known, the surface of a film of liquid in a dispersed-annular flow is covered by a complex system of waves. Two main types of waves with fundamentally different characteristics (formed by different mechanisms) can be distinguished: frequent ripples of relatively low amplitude having a three-dimensional structure; relatively infrequent shock waves with a large amplitude and a two-dimensional structure. The study [3] proposed a method of determining the mean thickness of the film without allowing for the shock waves. We used this method to analyze our data. The method is based on the assumption that the film-thickness distribution function should be symmetrical without allowance for the shock waves, and the abscissa of the maximum will be the mean thickness of the film if the film contains only

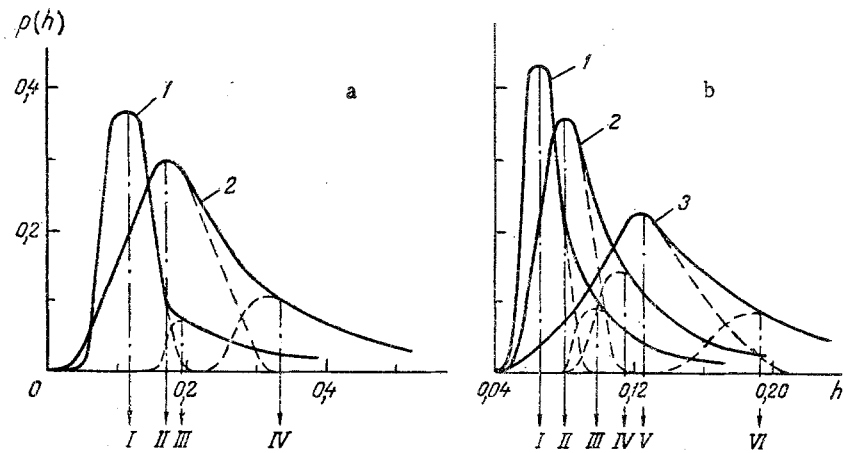


Fig. 1. Film-thickness distribution function in relation to the regime parameters: a)  $W_g = 15$  m/sec: 1)  $G_{fi} = 4 \cdot 10^{-3}$  kg/sec; 2)  $21 \cdot 10^{-3}$ ; b)  $G_{fi} = 15 \cdot 10^{-3}$  kg/sec: 1)  $W_g = 15$  m/sec; 2) 28; 3) 36; I)  $\langle h_r^1 \rangle$ , II)  $\langle h_r^2 \rangle$ , III)  $\langle h_{cs}^1 \rangle$ , IV)  $\langle h_{cs}^2 \rangle$ , V)  $\langle h_r^3 \rangle$ , VI)  $\langle h_{cs}^3 \rangle$ .  $h$ , mm.

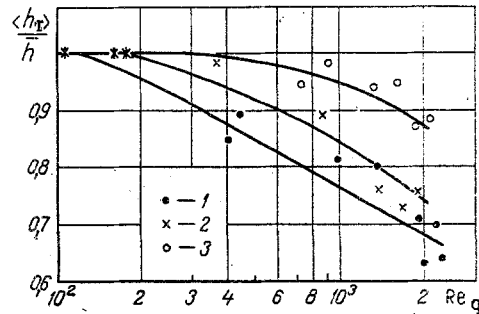


Fig. 2. Dependence of the ratio  $\langle h_r/\bar{h} \rangle$  on the dimensionless velocity of liquid in the flow for different values of  $Re_g$  (the boundary of the shock waves on the film surface according to the data in [8] is indicated by \*): 1)  $Re_g = 1.5 \cdot 10^4$ ; 2)  $3.0 \cdot 10^4$ ; 3)  $4.0 \cdot 10^4$ .

ripples  $\langle h_r \rangle$ . The distribution function of film thickness at the crests of the shock waves is obtained by geometric subtraction of the curve symmetrical relative to  $\langle h_r \rangle$  from the distribution function obtained from the histogram. These functions are shown in Fig. 1.

It is evident from the curves in Fig. 1 that with a constant gas velocity, the maximum of the distribution function is shifted to the region of greater film thicknesses with an increase in the velocity of the liquid in the film. This is accompanied by an increase in the range of  $h$  and the most probable film thickness at the crests of the shock waves. A similar pattern is seen with a constant liquid velocity in the film when gas velocity decreases.

Values of  $\langle h_r \rangle$  found from the graphs were compared with the mean film thickness calculated from the relation

$$\bar{h} = \frac{1}{N} \sum_{i=1}^N h_i,$$

where  $N = 100$ .

In all of the regimes investigated, the values of  $\langle h_r \rangle$  were less than  $\bar{h}$ . Meanwhile, the difference was greater, the greater the mean thickness of the film. This is evidently connected with the more complex structure of the surface of thick liquid films, expressed in greater asymmetry of the distribution curves of the data relative to  $\langle h_r \rangle$ . The character of the dependence of  $\langle h_r \rangle$  on liquid velocity in the film and gas velocity is similar to that established in [4, 5, etc.], although the absolute values of  $\langle h_r \rangle$  in our tests were lower

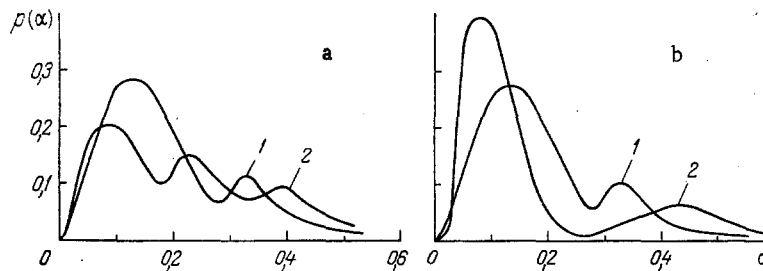


Fig. 3. Distribution function of the relative amplitude of waves on the film surface in relation to the regime parameters: a)  $W_g = 15$  m/sec; 1)  $G_{fi} = 15 \cdot 10^{-3}$  kg/sec; 2)  $25 \cdot 10^{-3}$ ; b)  $G_{fi} = 15 \cdot 10^{-3}$  kg/sec; 1)  $W_g = 15$  m/sec; 2) 28.

due to the lower velocities of the film liquid. It can be seen from Fig. 2 that the ratio  $\langle h_r \rangle / h$  decreases with an increase in the dimensionless velocity of the film liquid in the flow  $Re_q$  for different values of the Reynolds number  $Re_g$ , which is evidence of the increasing contribution of shock waves to the wave-formation process.

In connection with the fact that the absolute height of the perturbations on the film change within a fairly broad range, we can obtain more reliable data on the type of waves that cover its surface by using the concept of the relative amplitude of the waves:

$$\alpha = \frac{h_{\max} - h_{\min}}{h_{\max} + h_{\min}} = \frac{A}{\langle h \rangle}.$$

Figure 3 shows the effect of regime parameters on the form of the distribution function of relative wave amplitude. The curves have distinct maxima, these maxima being two or three in number. There are three maxima in the regimes in which liquid velocity in the film is greater for the same given gas velocity. The first maximum corresponds to the values of the relative amplitude of the ripples  $\alpha_r$ , which in our experiments lie within the range 0.05–0.2 ( $\alpha_r = 0.1$ –0.2 [3],  $\alpha_r = 0.25$  [6]).

Some studies which have examined wave formation on the surface of thin liquid films [6] have detected not only shock waves and ripples, but also so-called large waves. These waves are transitional between the ripples and the shock waves. They are distinguished by an amplitude considerably greater than the amplitude of the ripples. However, they still have a three-dimensional structure. The merging of several large waves may lead to the formation of a shock wave, which occupies the entire perimeter of the channel. Since the sensors recording the instantaneous thickness of the film were located along one generatrix of the channel, we were not able to distinguish between large waves and shock waves in our study.

The presence of the second and third maxima of the distribution function of relative amplitude can be explained by the existence of both two- and three-dimensional waves of large amplitude. Also, in [7] for example, investigators noted the multimodal character of shock waves on the surface of a flowing film at Reynolds numbers for the liquid greater than 700. These factors, along with the possible effect of gravity on wave formation in thick films with relatively low air velocities ( $W_g \approx 15$ –20 m/sec), explain the appreciable scatter of the data on thickness and the amplitude of the shock waves. For instance, the ratio  $\langle h_{cs} \rangle / \langle h_r \rangle$  (see Fig. 1) lies within the range 1.5–3.0. The ratio of the wave amplitude corresponding to the second maximum of the relative-amplitude distribution function to the amplitude of the ripples (first maximum) ranges from 1.5 to 6.0 (in [7], this ratio was equal to about 3.0).

The data obtained agrees well qualitatively with the results of spectral analysis of the film-thickness oscillograms [1]. The two methods of analyzing oscillograms complement each other and make it possible to obtain complete information on the amplitude–frequency characteristics of a liquid film in a dispersed-annular flow.

#### NOTATION

$G_q$ , velocity of liquid (water);  $W_g$ , velocity of gas (air);  $h$ , thickness of liquid film;  $\bar{h}$ , mean film thickness;  $\langle h_r \rangle$ , mean thickness of film in the presence of ripples on the film;  $\langle h_{cs} \rangle$ , mean thickness of film at crests of shock waves;  $h_{\max}$ ,  $h_{\min}$ , film thickness at crests

and troughs of the waves, respectively;  $k$ , number of intervals of grouping in the histogram construction;  $N$ , number of values of instantaneous film thickness recorded on the oscillogram;  $p(h)$ , film-thickness distribution function;  $p(\alpha)$ , relative-wave-amplitude distribution function;  $G_{fi}$ , film velocity in the film;  $Re_{fi} = G_{fi}/(\pi d\mu)$ , dimensionless velocity of liquid in the film;  $Re_q = 4G_q/(\pi d\mu)$ , dimensionless velocity of liquid in the flow;  $\mu$ , absolute viscosity;  $d$ , channel diameter;  $Re_g = W_g d/\mu_g$ , Reynolds number of gas;  $\nu_g$ , kinematic viscosity of gas.

#### LITERATURE CITED

1. N. D. Agafonova, "Development of a method of calculating fluid dynamics and drop mass transfer for high vapor contents in the tubular heating surfaces of steam generators to increase reliability of operation," Author's Abstract of Candidate's Dissertation, Engineering Sciences, Leningrad (1983).
2. J. S. Bendat and A. G. Piersol, Random Data: Analysis and Measurement Procedures, Wiley (1971).
3. K. J. Chu and A. E. Dukler, AIChE J., 20, No. 4, 695-706 (1974).
4. D. E. Woodmansee and T. J. Hanratty, AIChE J., 15, No. 3, 712-715 (1969).
5. T. Tomida and T. Okazaki, J. Chem. Eng. Jpn., 7, No. 5, 329-333 (1974).
6. N. A. Nikolaev, A. D. Sergeev, L. P. Kholpanov, et al., Teor. Osn. Khim. Tekhnol., 9 No. 3, 406-411 (1975).
7. K. J. Chu and A. E. Dukler, AIChE J., 21, No. 3, 583-593 (1975).
8. K. Sekoguchi, K. Hori, M. Nakazatomi, K. Nakano, and K. Nishikawa, Bull. ISME, 20, No. 145, 844-851 (1977).